

# The structural basis of urea-induced protein unfolding in $\beta$ -catenin

Chao Wang,<sup>a‡</sup> Zhongzhou Chen,<sup>a‡</sup> Xia Hong,<sup>a</sup> Fangkun Ning,<sup>a</sup> Haolin Liu,<sup>a</sup> Jianye Zang,<sup>a</sup> Xiaoxue Yan,<sup>a</sup> Jennifer Kemp,<sup>a</sup> Catherine A. Musselman,<sup>b</sup> Tatinna G. Kutateladze,<sup>b</sup> Rui Zhao,<sup>c</sup> Chengyu Jiang<sup>d\*</sup> and Gongyi Zhang<sup>a\*</sup>

<sup>a</sup>The Integrated Department of Immunology, National Jewish Health, Denver, CO 80206, USA, <sup>b</sup>Department of Pharmacology, Anschutz Medical Campus, University of Colorado, Aurora, CO 80045, USA, <sup>c</sup>Department of Biochemistry and Molecular Genetics, Anschutz Medical Campus, University of Colorado, Aurora, CO 80045, USA, and <sup>d</sup>Chinese Academy of Medical Sciences, Department of Biochemistry and Molecular Biology, Peking Union Medical College, Tsinghua University, Beijing 100005, People's Republic of China

‡ These authors contributed equally to this work.

Correspondence e-mail:  
chengyujiang@gmail.com, zhangg@njc.org

Although urea and guanidine hydrochloride are commonly used to denature proteins, the molecular underpinnings of this process have remained unclear for a century. To address this question, crystal structures of  $\beta$ -catenin were determined at various urea concentrations. These structures contained at least 105 unique positions that were occupied by urea molecules, each of which interacted with the protein primarily *via* hydrogen bonds. Hydrogen-bond competition experiments showed that the denaturing effects of urea were neutralized when polyethylene glycol was added to the solution. These data suggest that urea primarily causes proteins to unfold by competing and disrupting hydrogen bonds in proteins. Moreover, circular-dichroism spectra and nuclear magnetic resonance (NMR) analysis revealed that a similar mechanism caused protein denaturation in the absence of urea at pH levels greater than 12. Taken together, the results led to the conclusion that the disruption of hydrogen bonds is a general mechanism of unfolding induced by urea, high pH and potentially other denaturing agents such as guanidine hydrochloride. Traditionally, the disruption of hydrophobic interactions instead of hydrogen bonds has been thought to be the most important cause of protein denaturation.

Received 16 June 2014  
Accepted 7 August 2014

**PDB references:**  $\beta$ -catenin,  
4ev8; 4ev9; 4eva; 4evp; 4evt

## 1. Introduction

More than ten years ago, the examination of the structure of RNA polymerase from *Thermus aquaticus*, a species of bacterium that tolerates high temperatures, that we determined raised the question of what molecular and chemical forces stabilize the individual subunits and hold the complex together at temperatures greater than 70°C (Zhang *et al.*, 1999). At the time, it was commonly believed that thermostable proteins must contain extensive hydrophobic cores that stabilize their tertiary structures. Subsequent research, however, has failed to identify significant hydrophobic cores within proteins expressed by thermophilic bacteria (Zhang *et al.*, 1999). Thermophilic proteins do not have hydrophobic cores that are more extensive than those of mesophilic proteins. To examine this apparent discrepancy and to illustrate the primary stabilizing force in the tertiary structure of proteins, we have employed an experimental system that addresses how proteins are denatured by urea.

Urea and guanidine hydrochloride have been widely used as protein denaturants for a century. Although the way in which these denaturants catalyze protein unfolding has been extensively studied dating back to the 1930s (Wu, 1931; Mirsky & Pauling, 1936), the precise mechanism is still not completely

understood. At least three models have been proposed to explain this process. One common theory, referred to as the indirect or chaotropic mechanism, proposes that urea acts as a chaotrope, altering the hydrogen-bond structure of water and thus diminishing the effects of hydrophobic interactions and promoting the solvation of hydrophobic groups (Franks & Franks, 1968; Finer *et al.*, 1972; Bennion & Daggett, 2003; Watlauffer *et al.*, 1964; Barone *et al.*, 1970; Horwich & Willison, 1993). The second model states that van der Waals interactions between urea and hydrophobic moieties of either amino-acid side chains or the peptide backbone drive urea-induced denaturation (Prakash *et al.*, 1981; Timasheff & Xie, 2003; Lee & van der Vegt, 2006; Zangi *et al.*, 2009; Hua *et al.*, 2008; Stumpe & Grubmüller, 2007; Tsai *et al.*, 1996; Tanford, 1970; Nozaki & Tanford, 1963; Alonso & Dill, 1991; Zou *et al.*, 1998; Ikeguchi *et al.*, 2001; Duffy *et al.*, 1993; Bennion & Daggett, 2003; Caballero-Herrera *et al.*, 2005). Finally, Mirsky and Pauling hypothesized that hydrogen bonds between the protein, primarily its side chains, and urea will act to denature or unfold proteins (Mirsky & Pauling, 1936). This mechanism, which was extended by including hydrogen bonds between the protein backbone and urea, has been supported by a number of studies over the last several decades (Robinson & Jencks, 1965; Creighton, 1991; Oostenbrink & van Gunsteren, 2005; O'Brien *et al.*, 2007; Makhatadze & Privalov, 1992; Mountain & Thirumalai, 2003; Klimov *et al.*, 2004; Auton *et al.*, 2007).

Here, we have examined the crystal structure of  $\beta$ -catenin in the presence of various concentrations of urea, interactions between urea and polyethylene glycol (PEG), and protein unfolding at high pH to obtain direct evidence of which of these mechanisms best explains the effects of urea.

## 2. Materials and methods

### 2.1. Expression, purification and crystallization

The purification protocol of a cDNA fragment encoding amino-acid residues 137–674 of murine  $\beta$ -catenin ( $\beta$ 59) has previously been described by Huber *et al.* (1997). Briefly, the cell lysates were loaded onto glutathione–agarose beads (Sigma), which were then extensively washed with resuspension buffer. In-gel digestion was performed overnight at 4°C using thrombin. Digested  $\beta$ 59 was further purified using anion-exchange (MonoQ; GE Healthcare Life Sciences) and size-exclusion chromatography (Superdex 200; GE Healthcare Life Sciences). The protein was concentrated to 7 mg ml<sup>-1</sup> in buffer consisting of 10 mM CAPS pH 10.5, 50 mM NaCl, 1 mM DTT. Crystals of  $\beta$ 59 were obtained using the hanging-drop vapor-diffusion method at 4°C over a reservoir solution consisting of 200 mM Tris–HCl pH 8.5, 2.4–3.0 M urea.

### 2.2. Crystallization with increasing urea concentrations and crystal cross-linking

Two approaches were used to increase the urea concentration. Firstly, the crystals were directly transferred into equilibrated drops with urea concentrations of 4.0, 5.6 and 6.4 M in addition to 200 mM Tris–HCl pH 8.5. Further equi-

libration was carried out for at least 2 h. When the urea concentration was increased to 7.2 M, however, the crystals disappeared within 30 min. In the second approach, the crystals were cross-linked with 25% glutaraldehyde and the urea concentration was then raised to 7.2 or 8.3 M as described for the first approach (Supplementary Fig. S3<sup>1</sup>). Crystal cross-linking was performed following the protocols described by Lusty (1999). The cross-linking reaction should not exceed 24 h or the crystal will no longer diffract. After cross-linking, the  $\beta$ 59 crystals could be placed in 8.3 M urea for several hours.

### 2.3. Data collection, data processing and model refinement

Crystals from drops containing different urea concentrations were dipped into cryoprotectant (urea and 20% glycerol) for several seconds and cooled in liquid nitrogen. All data were collected at 100 K on beamline 8.2.2 at the Advanced Light Source, Berkeley, California, USA. Data-collection statistics are shown in Supplementary Table S1. Data were integrated and scaled with the *HKL-2000* software package (Otwinowski *et al.*, 2003). All structures were determined using differential Fourier maps with the published  $\beta$ 59 structure (PDB entry 3bct; Huber *et al.*, 1997) as the initial model. The *CCP4* suite and *CNS* were used for all refinements (Winn *et al.*, 2011; Brünger *et al.*, 1998). Model-refinement statistics can be found in Supplementary Table S2. We used the  $F_o - F_c$  and  $2F_o - F_c$  maps to assign and confirm the position of a given urea molecule. If we found no negative density when placing a urea molecule and found more positive density when placing a water molecule, we assigned this position as a urea. Otherwise, we assigned the position as a water molecule.

### 2.4. Measurement of circular-dichroism (CD) spectra using buffers at different pH values

Native  $\beta$ 59 was diluted to a final concentration of 0.1 mg ml<sup>-1</sup> in various buffers of pH 8.5, 9.5, 10.5, 11.5, 12.0, 12.5 or 13.0 (Supplementary Table S3). The CD spectrum of each sample was measured using a Jasco J-815 spectropolarimeter (Biophysics Core Facility, University of Colorado Denver, USA). CD spectra were obtained for two additional denatured samples treated with 8 M urea as unfolded control samples.

### 2.5. Binding energy between urea and amide or polyethylene glycol (PEG)

Urea, water, amide, PEG analogs and their complexes were defined as the reactants and were optimized at the B3LYP/6-31G(d,p) level (Becke, 1993; Wu & Lai, 1995) using *Gaussian* 98 (Frisch, 1998). Frequency calculations were performed for each optimized structure. Zero-point vibrational corrections and thermal corrections were used as the energy values at the B3LYP/6-31G(d,p) level. The relative energies of the hydrogen bond refer to the difference between the energies

<sup>1</sup> Supporting information has been deposited in the IUCr electronic archive (Reference: QH5012).

and the corresponding complex. BSSE energy corrections were calculated using the counterpoise method (Simon *et al.*, 1996).

## 2.6. Crystallization with and without PEG 8K

The original crystallization conditions using urea as the precipitant included an additional 0.5% PEG 8K in the reservoir solution. To investigate the ability of PEG to neutralize urea, parallel crystallization drops with and without PEG 8K (Fluka) in the reservoir solution were created, whereas all other components in the drops were kept constant. Briefly, 3.0–8.0 M urea was used as the precipitant, 200 mM Tris–HCl pH 8.5 was used as a buffer and a gradient concentration of PEG 8K from 1.0 to 7.0% was used for each urea concentration. All drops were placed at 4°C for several days and then checked for crystals.

## 2.7. PCR with and without PEG 8K

PCR experiments were performed using 50 µl reactions and standard conditions (Supplementary Tables S4 and S5). *Taq* polymerase, PCR buffer and dNTPs were purchased from Invitrogen. The template used for these experiments was approximately 530 bp in length. PCR products were assayed by electrophoresis on 1.0% agarose gels.

## 2.8. Nuclear magnetic resonance spectroscopy

The acetyl-4-polyglycine (Ac-GGGG) peptide was dissolved in 1× PBS buffer and one-dimensional <sup>1</sup>H NMR spectra were obtained at various pH values (8.5–13) using the *BioPack* 3919 Watergate sequence on a Varian Inova 500 MHz spectrometer. Spectra were processed and analyzed using *NMRPipe*; all peaks were referenced to DSS.

## 3. Results and discussion

### 3.1. Structural determination

As crystals of  $\beta$ -catenin protein were obtained using 2.4 M urea as precipitant as reported and several urea molecules were identified to interact with the protein (Huber *et al.*, 1997), we speculate that more urea molecules could be found by increasing the urea concentration. In this regard, a  $\beta$ -catenin protein-expression vector which encoded the core region (residues 134–671; 12 copies of a 42-amino-acid motif called the armadillo repeat domain) was expressed and purified as previously described (Huber *et al.*, 1997). The purified protein was crystallized using only urea as a precipitant without PEG to avoid the neutralization effect described below.  $\beta$ -Catenin crystals were first obtained using 2.4 M urea and 200 mM Tris–HCl buffer pH 8.5. The urea concentration in these crystals was then increased by soaking them in 4.0 or 5.6 M urea. To increase the concentrations of urea still further, the  $\beta$ -catenin crystals were cross-linked with glutaraldehyde prior to soaking in 7.2 or 8.3 M urea. All crystals belonged to the same space group,  $C222_1$  (Huber *et al.*, 1997), with the exception of the crystal obtained with 5.6 M urea, which belonged to space group  $C2$ . All five structures were determined using difference Fourier maps (Brünger *et al.*, 1998) and previously published coordinates (PDB entry 3bct) as the initial model at 1.9–2.4 Å resolution (Fig. 1). In all five complexes we identified triangular electron density reflecting the shape of urea molecules (Fig. 2). Details of the methods for crystallization, soaking the crystals in high-concentration urea, data collection, structural determination and refinement can be found in §2 and Supplementary Table S1.

### 3.2. Overall structures of $\beta$ -catenin and urea

In the final refined models, the structures of  $\beta$ -catenin in all five complexes were fairly similar, with the exception of minor differences in the N-terminal regions (Supplementary Fig. S1). On the other hand, the mean temperature factors increased from 37.4 Å<sup>2</sup> in the crystal structure obtained with 2.4 M urea to 67.3 Å<sup>2</sup> in the crystal structure obtained with 8.3 M urea

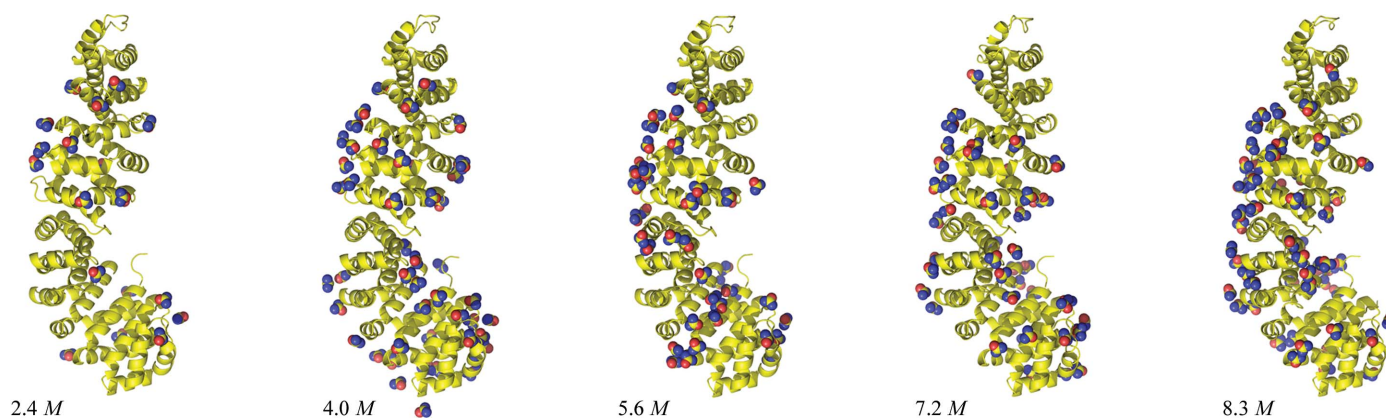


**Figure 1**

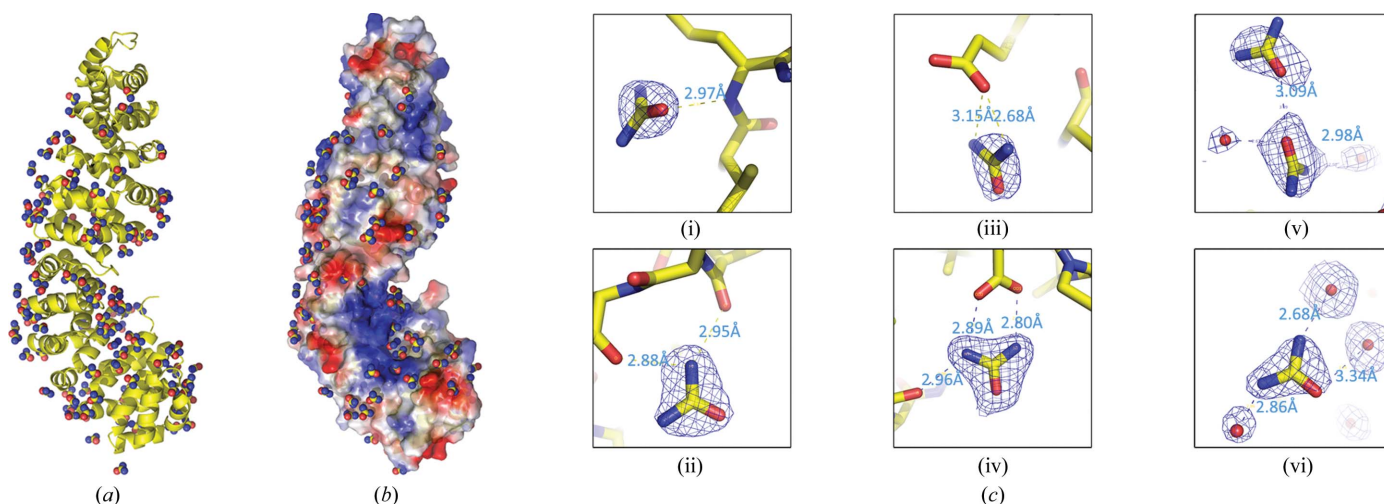
Complex structures of  $\beta$ -catenin at different urea concentrations. Shown are the urea molecules which were found in the models. From low concentration to high, 2.4, 4.0, 5.6, 7.2 and 8.3 M, respectively, there were 19, 49, 42, 44 and 56 urea molecules in each model.  $\beta$ -Catenin, yellow; urea N atoms, blue; urea C atoms, yellow; urea O atoms, red.

(Supplementary Table S2). 19 urea molecules were detected in the  $\beta$ -catenin structure obtained with 2.4 M urea, whereas 49, 42, 44 and 56 urea molecules were observed with 4.0, 5.6, 7.2 and 8.3 M urea, respectively (Supplementary Table S2). Interestingly, at different urea concentrations the urea molecules occupied different positions on the surface of  $\beta$ -catenin (Fig. 1). Combining all of the positions occupied by urea molecules in the five complexes, 105 unique urea molecules were identified on the surface of  $\beta$ -catenin (Fig. 2). Surpris-

ingly, the surface-charge distribution on  $\beta$ -catenin showed that all of the urea molecules were distributed on hydrophilic surfaces (Fig. 2).

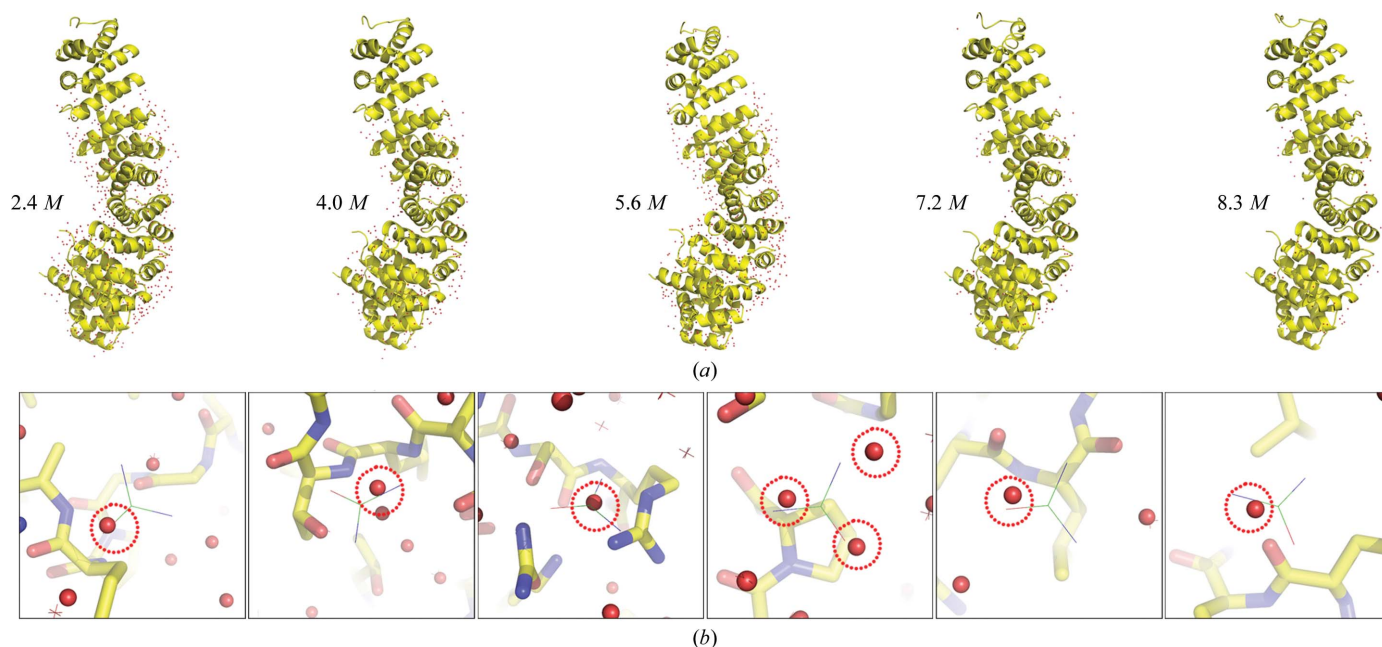
### 3.3. Modes of interaction in the structures

We then performed a detailed analysis of the interactions between urea molecules and the protein, other urea molecules or water molecules. Several major interaction modes were



**Figure 2**

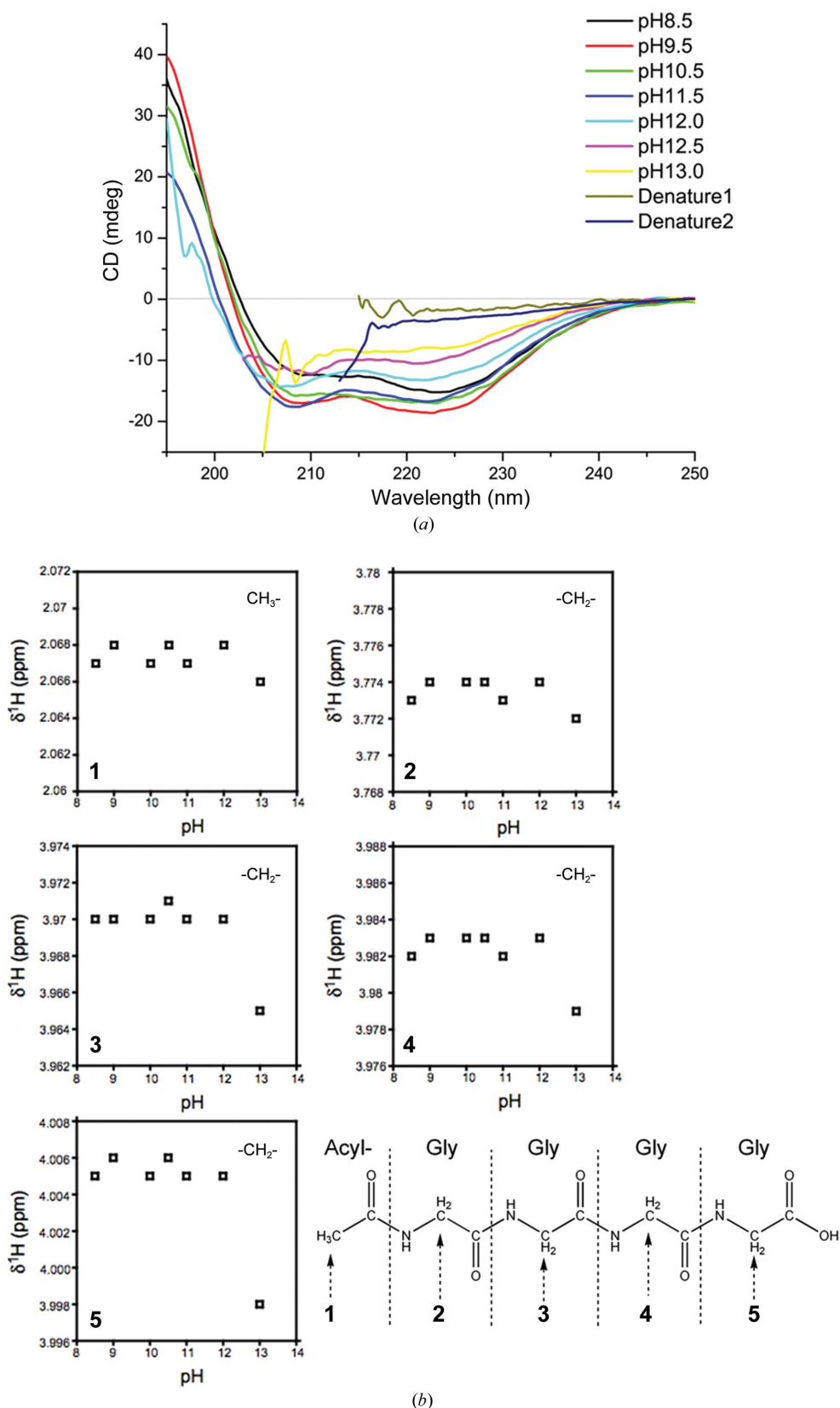
Urea binds to hydrophilic surfaces in  $\beta$ -catenin primarily through hydrogen bonds. (a) The distribution of all 105 non-overlapping urea molecules on the surface of  $\beta$ -catenin surrounding the  $\beta$ -catenin molecule, colored as in Fig. 1. (b) All urea molecules are close to the hydrophilic surface of  $\beta$ -catenin: positively charged surfaces are shown in blue, negatively charged surfaces in red and neutral or hydrophobic surfaces in white. Urea molecules are colored as in Fig. 1. (c) Urea molecules forming (i) hydrogen bonds with main-chain amide groups, (ii) hydrogen bonds with main-chain carboxyls, (iii, iv) hydrogen bonds with side chains, (v) hydrogen bonds with each other and (vi) hydrogen bonds with water. Urea molecules (triangular stars) are covered in  $2F_o - F_c$  electron density (blue) with a  $2\sigma$  cutoff. Waters are shown as red dots.



**Figure 3**

The structure of water in the  $\beta$ -catenin complexes. (a) Water-molecule distribution within the complexes of protein at different urea concentrations. The number of water molecules decreases with increasing urea concentration. (b) Water molecules in the dotted circles were replaced by urea molecules in different complexes. Red dots, water molecules; triangular stars, urea molecules.




**Figure 5**

The protein unfolds and protons dissociate from the peptide at high pH values. (a)  $\beta$ -Catenin unfolding at pH 12.5 or greater was detected using CD spectra. Denature1 indicates sample prepared at 8 M urea after overnight incubation; Denature2 indicates sample prepared from Denature1 with an additional 15 min of heating at 100°C. (b) Dissociation of protons from the amide of Ac-GGGG at pH 13 was detected based on the NMR chemical shifts of neighboring H atoms.

obtained at 8.3 M urea and 2.4 Å resolution. Nevertheless, water molecules were replaced by urea molecules in each of the five structures in comparison to the reported structure (Fig. 3; Huber *et al.*, 1997). In some cases one urea molecule replaced one water molecule, although in others two or more water molecules were displaced (Fig. 3b). Among all five complex structures, 105 water molecules were replaced by urea molecules on the protein surface. It appears that urea molecules only compete with water molecules in interacting with the protein molecule.

### 3.5. Hydrogen-bond competition experiments with PEG

As mentioned earlier, one of the proposed theories suggests that urea and guanidine hydrochloride unfold proteins *via* a chaotropic effect, meaning that the layer structure of water molecules on the protein surface is disrupted, exposing hydrophobic areas and collapsing the tertiary structure (Finer *et al.*, 1972; Franks & Franks, 1968). The complex structures of  $\beta$ -catenin and urea showed that water molecules were replaced by urea molecules; no urea molecules were found to interact with hydrophobic moieties on the surface of  $\beta$ -catenin. Instead, higher urea concentrations resulted in more direct binding of urea molecules to the protein through hydrogen bonds. These data argue against the chaotropic mechanism for urea-induced protein unfolding.

We performed a hydrogen-bond competition experiment to confirm that disruption of hydrogen bonds within protein atoms by urea molecules was the primary denaturing factor. Our calculations suggested that PEG is a strong hydrogen-bond acceptor (Fig. 4). Under ideal conditions (gas phase), a

hydrogen bond between urea and PEG produces 26.14 kJ mol<sup>-1</sup> of free energy, whereas a hydrogen bond between a main-chain carbonyl O atom and urea only produces 23.32 kJ mol<sup>-1</sup> of free energy (Fig. 4a). Thus, in solution, PEG should compete with proteins for urea binding. Indeed, a mutant version of the sTALL-1 protein (mTALL-1) which was unable to form protein clusters (Liu *et al.*, 2002) was crystallized in 2.0 M urea. Gradually increasing the urea concentration from 3.0 to 4.0, 5.0, 6.0, 7.0 and 8.0 M prevented the formation of mTALL-1 crystals. When an appropriate concentration of PEG 4K was added to the crystallization buffer, however, crystals of mTALL-1 were again obtained (Fig. 4b).

Because urea was used as the precipitant for crystallization, our calculations suggested that 8 M urea would not be completely neutralized by 6% PEG 8K if one urea molecule bound to one polyglycol unit. Therefore, we employed a more sensitive DNA polymerase chain reaction (PCR)-based system to verify the neutralization effect of PEG on urea. The formation of hydrogen bonds between complementary DNA chains during primer pairing and chain elongation, along with nucleotide ligation on the newly synthesized chain, are critical steps in the PCR process. Urea completely disrupted PCR even at very low concentrations (0.96 M; Fig. 4c). Importantly, this disruption was abolished by the addition of PEG 4K (Fig. 4c). The amount of PEG required to neutralize the effects of urea completely in these experiments suggested that at least two glycol units were required for each urea molecule. Since PEG binds to urea *via* hydrogen bonds and thus should compete with the binding of urea to proteins *via* the same mechanism, these data support the model in which disruption of hydrogen bonds in proteins is the primary factor that causes proteins to unfold in the presence of urea.

### 3.6. Protein unfolding at high pH

We then examined protein unfolding in high-pH solutions because hydrogen bonds are known to be very sensitive to pH changes. Analysis of CD spectra (Greenfield & Fasman, 1969) showed that  $\beta$ -catenin remains stable at pH levels as high as 12.5 and disruption of secondary structures was observed starting at a pH of 13.0 (Fig. 5a). To confirm that the protein unfolding detected at high pH was caused by a breakdown of hydrogen bonds, an N-terminally acetylated polyglycine peptide (Ac-GGGG) was examined at high pH using NMR spectroscopy. As reported previously (Udgaonkar & Baldwin, 1988; Bai *et al.*, 1993), the exchange rate of the hydrogen on the amide moiety markedly increased at high pH, although it is difficult to detect the chemical shifts of these H atoms on amides. Dissociation of these protons, however, could cause chemical shifts in neighboring H atoms, including those from the CH<sub>3</sub> group or the four CH<sub>2</sub> groups of Ac-GGGG, owing to hydrogen coupling of these atoms with the amide moieties. Importantly, we observed significant chemical shifts within Ac-GGGG at pH 13 (Fig. 5b). These data suggested that at pH 13 the amide protons were able to dissociate (Fig. 5b), a result that is consistent with hydrogen-bond disruption even though

the theoretical pK<sub>a</sub> value of the amide protons is ~15–17 (Gilli *et al.*, 2009). These data suggest that the atomic mechanism driving protein unfolding under high pH conditions is similar to the mechanism underlying urea-induced denaturation and that both are characterized by the disruption of hydrogen bonds in the proteins, most of which are normally found within protein backbones.

The unfolding of proteins by urea and guanidine hydrochloride has been a focus of research for many decades. Different theories have been introduced to explain the underlying mechanism, although none of these has been validated by direct experimental data. Our observations of direct interactions between proteins and urea molecules, competition data obtained with PEG, CD spectra and NMR experiments performed at high pH help to elucidate the molecular underpinnings of this process. Moreover, our results may have broader implications. For example, hydrogen bonds may play a more important role in stabilizing the tertiary structures of proteins from thermophilic bacteria. This conclusion may also translate to the vast majority of native proteins.

We thank John Kappler, Philippa Marrack, James Hurley, Robert Stroud, Brian Matthews and Seth Darst for reading the manuscript and James Kappler for editing the manuscript before submission. We thank William Weis for the  $\beta$ -catenin expression vector, Lei Yin and Shaodong Dai for help in data collection and The Howard Hughes Medical Institute, the Zuckerman/Canyon Ranch and Alan Lapporte for supporting the X-ray and computing facilities. All X-ray data sets were collected on the Howard Hughes Medical Institute beamlines 8.2.1 and 8.2.2 at the Advanced Light Source, Berkeley, California, USA. CD data and NMR data were obtained at the core facility of University of Colorado Denver. This work was inspired by the research of Hsien Wu in the 1930s, by the complete synthesis of bovine insulin by a group of Chinese scientists in the 1960s and by the encouragement of Professor Dongcai Liang. This work was supported by the following grants: a Chinese 111 project (B08007), NIH grant AI22295 and NIH grant GM80719.

### References

- Alonso, D. O. & Dill, K. A. (1991). *Biochemistry*, **30**, 5974–5985.  
 Auton, M., Holthausen, L. M. & Bolen, D. W. (2007). *Proc. Natl Acad. Sci. USA*, **104**, 15317–15322.  
 Bai, Y., Milne, J. S., Mayne, L. & Englander, S. W. (1993). *Proteins*, **17**, 75–86.  
 Barone, G., Rizzo, E. & Vitagliano, V. (1970). *J. Phys. Chem.* **74**, 2230–2232.  
 Becke, A. D. (1993). *J. Chem. Phys.* **98**, 5648–5652.  
 Bennion, B. J. & Daggett, V. (2003). *Proc. Natl Acad. Sci. USA*, **100**, 5142–5147.  
 Brünger, A. T., Adams, P. D., Clore, G. M., DeLano, W. L., Gros, P., Grosse-Kunstleve, R. W., Jiang, J.-S., Kuszewski, J., Nilges, M., Pannu, N. S., Read, R. J., Rice, L. M., Simonson, T. & Warren, G. L. (1998). *Acta Cryst. D* **54**, 905–921.  
 Caballero-Herrera, A., Nordstrand, K., Berndt, K. D. & Nilsson, L. (2005). *Biophys. J.* **89**, 842–857.  
 Creighton, T. E. (1991). *Curr. Biol.* **1**, 8–10.

- Duffy, E. M., Kowalczyk, P. J. & Jorgensen, W. L. (1993). *J. Am. Chem. Soc.* **115**, 9271–9275.
- Finer, E. G., Franks, F. & Tait, M. J. (1972). *J. Am. Chem. Soc.* **94**, 4424–4429.
- Franks, H. S. & Franks, F. (1968). *J. Chem. Phys.* **48**, 4746–4757.
- Frisch, M. J. *et al.* (1998). *Gaussian 98*. Gaussian Inc., Pittsburgh, Pennsylvania, USA.
- Gilli, P., Pretto, L., Bertolasi, V. & Gilli, G. (2009). *Acc. Chem. Res.* **42**, 33–44.
- Greenfield, N. & Fasman, G. D. (1969). *Biochemistry*, **8**, 4108–4116.
- Horwich, A. L. & Willison, K. R. (1993). *Philos. Trans. R. Soc. Lond. B Biol. Sci.* **339**, 313–325.
- Hua, L., Zhou, R., Thirumalai, D. & Berne, B. J. (2008). *Proc. Natl Acad. Sci. USA*, **105**, 16928–16933.
- Huber, A. H., Nelson, W. J. & Weis, W. I. (1997). *Cell*, **90**, 871–882.
- Ikeguchi, M., Nakamura, S. & Shimizu, K. (2001). *J. Am. Chem. Soc.* **123**, 677–682.
- Klimov, D. K., Straub, J. E. & Thirumalai, D. (2004). *Proc. Natl Acad. Sci. USA*, **101**, 14760–14765.
- Lee, M.-E. & van der Vegt, N. F. A. (2006). *J. Am. Chem. Soc.* **128**, 4948–4949.
- Liu, Y., Xu, L., Opalka, N., Kappler, J., Shu, H.-B. & Zhang, G. (2002). *Cell*, **108**, 383–394.
- Lusty, C. J. (1999). *J. Appl. Cryst.* **32**, 106–112.
- Makhatadze, G. I. & Privalov, P. L. (1992). *J. Mol. Biol.* **226**, 491–505.
- Mirsky, A. E. & Pauling, L. (1936). *Proc. Natl Acad. Sci. USA*, **22**, 439–447.
- Mountain, R. D. & Thirumalai, D. (2003). *J. Am. Chem. Soc.* **125**, 1950–1957.
- Nozaki, Y. & Tanford, C. (1963). *J. Biol. Chem.* **238**, 4074–4081.
- O'Brien, E. P., Dima, R. I., Brooks, B. & Thirumalai, D. (2007). *J. Am. Chem. Soc.* **129**, 7346–7353.
- Oostenbrink, C. & van Gunsteren, W. F. (2005). *Phys. Chem. Chem. Phys.* **7**, 53–58.
- Otwinowski, Z., Borek, D., Majewski, W. & Minor, W. (2003). *Acta Cryst.* **A59**, 228–234.
- Prakash, V., Loucheux, C., Scheufele, S., Gorbunoff, M. J. & Timasheff, S. N. (1981). *Arch. Biochem. Biophys.* **210**, 455–464.
- Robinson, D. R. & Jencks, W. P. (1965). *J. Am. Chem. Soc.* **87**, 2462–2470.
- Simon, S., Duran, M. & Dannenberg, J. J. (1996). *J. Chem. Phys.* **105**, 11024.
- Stumpe, M. C. & Grubmüller, H. (2007). *J. Am. Chem. Soc.* **129**, 16126–16131.
- Stumpe, M. C. & Grubmüller, H. (2008). *PLoS Comput. Biol.* **4**, e1000221.
- Tanford, C. (1970). *Adv. Protein Chem.* **24**, 1–95.
- Timasheff, S. N. & Xie, G. (2003). *Biophys. Chem.* **105**, 421–448.
- Tsai, J., Gerstein, M. & Levitt, M. (1996). *J. Chem. Phys.* **104**, 9417.
- Udgaonkar, J. B. & Baldwin, R. L. (1988). *Nature (London)*, **335**, 694–699.
- Watlauffer, D. B., Malik, S. K., Stoller, L. & Coffin, R. L. (1964). *J. Am. Chem. Soc.* **86**, 508–514.
- Winn, M. D. *et al.* (2011). *Acta Cryst.* **D67**, 235–242.
- Wu, H. (1931). *Chin. J. Physiol.* **5**, 321–334.
- Wu, Y.-D. & Lai, D. K. W. (1995). *J. Am. Chem. Soc.* **117**, 11327–11336.
- Zangi, R., Zhou, R. & Berne, B. J. (2009). *J. Am. Chem. Soc.* **131**, 1535–1541.
- Zhang, G., Campbell, E. A., Minakhin, L., Richter, C., Severinov, K. & Darst, S. A. (1999). *Cell*, **98**, 811–824.
- Zou, Q., Habermann-Rottinghaus, S. M. & Murphy, K. P. (1998). *Proteins*, **31**, 107–115.